Editors' Suggestion

Fractional Quantum Hall Effect Energy Gaps: Role of Electron Layer Thickness

K. A. Villegas Rosales, P. T. Madathil, Y. J. Chung, L. N. Pfeiffer, K. W. West, K. W. Baldwin, and M. Shayegan
Department of Electrical Engineering, Princeton University, Princeton, New Jersey 08544, USA

(Received 9 March 2021; accepted 24 June 2021; published 28 July 2021)

The fractional quantum Hall effect stands as a quintessential manifestation of an interacting two-dimensional electron system. One of the fractional quantum Hall effect's most fundamental characteristics is the energy gap separating the incompressible ground state from its excitations. Yet, despite nearly four decades of investigations, a quantitative agreement between the theoretically calculated and experimentally measured energy gaps is lacking. Here we report a systematic experimental study that incorporates very high-quality two-dimensional electron systems confined to GaAs quantum wells with fixed density and varying well widths. The results demonstrate a clear decrease of the energy gap as the electron layer is made thicker and the short-range component of the Coulomb interaction is weakened. We also provide a quantitative comparison between the measured energy gaps and the available theoretical calculations that takes into account the role of finite layer thickness and Landau level mixing. All the measured energy gaps fall below the calculations, but as the electron layer thickness increases, the results of experiments and calculations come closer. Accounting for the role of disorder in a phenomenological manner, we find better overall agreement between the measured and calculated energy gaps, although some puzzling discrepancies remain.

DOI: 10.1103/PhysRevLett.127.056801

The fractional quantum Hall effect (FQHE) [1–4] is one of the most celebrated many-body phenomena in condensed matter physics. It has been under study for nearly 40 years and has influenced other fields of physics beyond condensed matter [5]. It is observed in clean (low-disorder) two-dimensional electron systems (2DESs) when cooled to low temperatures and exposed to a large perpendicular magnetic field so that the thermal and kinetic (Fermi) energies are quenched, and electron-electron interaction dominates. The FQHE signals the formation of an incompressible liquid that has a quantized Hall resistance and flows without dissipation in the limit of zero temperature. It is also the first discovered topological state whose emergence requires interaction [6], and some FQHE states are indeed considered prime platforms for topological quantum computing [7–9].

The strongest and most basic FQHE is observed at Landau level (LL) filling factor $\nu = 1/3$ [1]. The physical properties of this state have been of continued fascination and research since its discovery [2–4,10–32]. Theoretical calculations predict an energy gap $^{1/3}\Delta = 0.10E_C$ for an "ideal" 2DES with zero layer thickness, no disorder, and an infinite separation between the LLs so that the ground state is formed entirely within the lowest LL [3,15–17]. The parameter $E_C = e^2/4\pi\epsilon_0\epsilon l_B$ is the Coulomb energy, where $l_B = \sqrt{\hbar/eB}$ is the magnetic length. The energy gaps measured in realistic, experimental samples, however, are smaller than the ideal value because the finite (nonzero) thickness of the electron layer, the proximity of the higher LLs, i.e., the ensuing LL mixing (LLM), and the ubiquitous disorder all tend to lower the energy gaps. Assessing the role of these factors, and a quantitative comparison of the measured and calculated $^{1/3}\Delta$, has been of interest for a long time. Experimentally, with improvements in sample quality, the measured energy gaps have generally increased [18–21]. On the theoretical side, realistic factors such as electron layer thickness [22–25], LLM [23,26,27], and disorder [28,29] have been considered to explain the experimental data. Nevertheless, the experimentally deduced gaps still fall bellow what theory predicts.

An important, experimentally controllable parameter that influences $^{1/3}\Delta$ is the thickness ($\tilde{w}$) of the electron layer. A larger $\tilde{w}$ weakens the short-range component of the electron-electron interaction and reduces $^{1/3}\Delta$. Despite its fundamental importance, systematic experimental measurements of $^{1/3}\Delta$ as a function of $\tilde{w}$ have been very scarce. Shayegan *et al.* [30] performed a study of $^{1/3}\Delta$ as a function of $\tilde{w}$ for an electron system confined to an AlGaAs quantum well (QW) with a parabolic potential profile. As the electron density (n) is varied in this system using gate bias, $\tilde{w}$ varies also. The measurements provided clear evidence that $^{1/3}\Delta$ decreases as $\tilde{w}$ increases, and eventually vanishes for sufficiently large values of $\tilde{w}$. Subsequent calculations [31,32] corroborated the experimental results qualitatively. However, there are two notable shortcomings in the measurements of Ref. [30]. First, since the 2DES resides in an AlGaAs QW, it suffers significantly from alloy disorder and therefore exhibits reduced gaps. Moreover, as the charge distribution is made wider by increasing n, the 2DES experiences more severe alloy disorder because the

electron wave function spreads more into a region with larger Al alloy fraction. Second, since the experiments are done by tuning n, the influence of LLM on $^{1/3}\Delta$ also changes as $\tilde{w}$ is increased. [The LLM parameter κ is defined as the ratio of the Coulomb energy and the LL separation: $\kappa = (e^2/4\pi\epsilon_0\epsilon l_B)/(\hbar eB/m^*)$, where m^* is the effective band mass. For a fixed ν, $\kappa \propto 1/\sqrt{n}$.]

Here we present a systematic experimental study of $^{1/3}\Delta$ versus $\tilde{w}$ in extremely high-quality 2DESs confined to modulation-doped GaAs QWs grown on GaAs (001) substrates. The QWs are flanked by 150-nm-thick $Al_{0.24}Ga_{0.76}As$ barriers, and the dopants are placed in doping wells [33]. The 2DESs all have the same density $n \simeq 1.1 \times 10^{11}$ cm^{-2}, in order to keep the LLM parameter fixed, and the QW widths (w) are varied from 20 to 80 nm to change $\tilde{w}$. We designate each sample by S_w; e.g., S_{20} refers to the sample with a QW of width $w = 20$ nm. The samples have a 4×4 mm^2 van der Pauw geometry, with alloyed InSn electrical contacts at the corners and edge midpoints. We used ^{3}He and dilution refrigerator systems, and conventional lock-in techniques to obtain magnetoresistance data, and determined $^{1/3}\Delta$ from the activated temperature dependence of the resistance minimum at $\nu = 1/3$. In addition, we measured the energy gaps for numerous higher-order FQHE states, and used the gaps to estimate values for disorder in each sample. All our measurements were done without illumination.

The extremely high quality of the samples is illustrated in Fig. 1(a), which shows the low-temperature ($T = 0.3$ K) mobility (μ) versus w. Except for S_{20}, for all samples μ exceeds 1×10^7 cm^2/V s despite the relatively small density. The enhancement in mobility with increasing w seen up to $w = 50$ (regions I and II) is related to the reduced role of interface roughness scattering [34,35]. When the 2DES is confined to a wider QW, the charge distribution penetrates the flanking $Al_{0.24}Ga_{0.76}As$ spacers to a smaller extent and the 2DES effectively experiences less alloy disorder. Once w exceeds 50 nm [region III in Fig. 1(a)], the 2DES starts to occupy the second electric subband, and the mobility drops precipitously because of the additional intersubband scattering [36].

In Figs. 1(b) and 1(c) we show the longitudinal resistance (R_{xx}) versus B for S_{20} and S_{30} at $T \simeq 25$ mK. Numerous minima observed in R_{xx} at fractional fillings $\nu = p/(2p+1)$, where p is an integer, attest to a plethora of FQHE states and the high quality of the samples. For S_{20} [Fig. 1(b)], we observe minima up to $\nu = 8/17$ ($p = 8$), while S_{30} [Fig. 1(c)] exhibits FQHE minima up to $\nu = 10/21$ ($p = 10$). This is consistent with the higher mobility of S_{30}. Data for samples with larger w, presented in the Supplemental Material (SM) [37], also show FQHE minima up to $p = 10$. In the insets of Figs. 1(b) and 1(c) we show Arrhenius plots of R_{xx} at $\nu = 1/3$ versus $1/T$, from which we determine $^{1/3}\Delta$ using fits of the form: $R_{xx} \propto \exp(-^{1/3}\Delta/2T)$. For S_{20} and S_{30}, $^{1/3}\Delta$ are (8.7 ± 0.1) and (8.0 ± 0.4) K, respectively. It is noteworthy that, despite its higher mobility and quality, S_{30} has the smaller $^{1/3}\Delta$, already hinting that a larger electron layer thickness leads to a smaller $^{1/3}\Delta$.

Figure 2 presents $^{1/3}\Delta$ (in units E_C) versus the effective layer thickness $\tilde{w}$ (in units of l_B); each data point is from a different 2DES whose QW width is given in the top axis. We use a Schrödinger-Poisson solver [38] to calculate the charge distribution in each QW self-consistently, and define $\tilde{w}$ as the standard deviation of the charge distribution from its center. Examples are shown in the insets of Fig. 2 for $w = 20$ and 70 nm. As seen in Fig. 2, $^{1/3}\Delta$ decreases with increasing $\tilde{w}$, establishing the qualitatively expected behavior from the softening of the Coulomb interaction in thicker

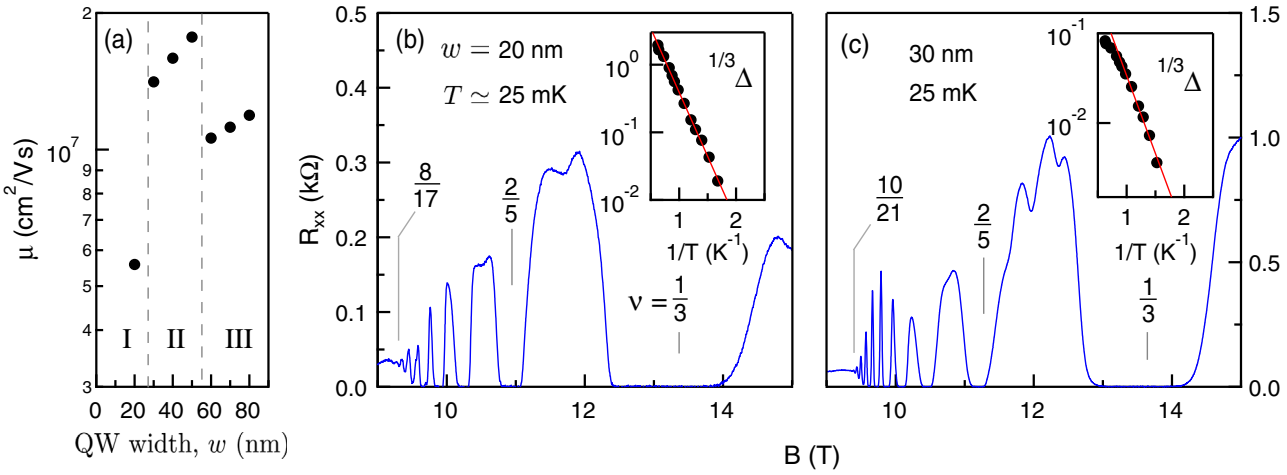

FIG. 1. (a) Transport mobility (μ) versus quantum well width (w). (b),(c) Longitudinal resistance (R_{xx}) versus perpendicular magnetic field (B) for GaAs 2DESs with density $\simeq 1.1 \times 10^{11}$ cm^{-2}, and $w = 20$ and 30 nm. The insets show the Arrhenius plots of R_{xx} minimum at $\nu = 1/3$ from which we deduce $^{1/3}\Delta$.

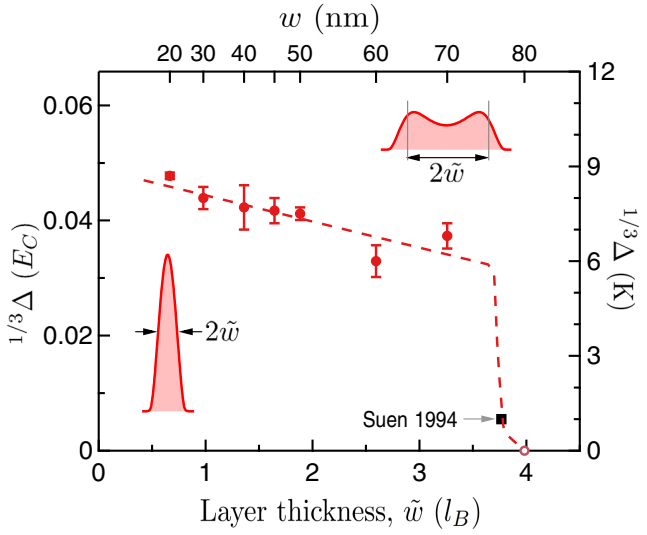

FIG. 2. $^{1/3}\Delta$ (in units of Coulomb energy E_C) versus effective layer thickness $\tilde{w}$ (in units of magnetic length l_B); in our samples $l_B \simeq 7.1$ nm at $\nu = 1/3$. We show the charge distributions (from self-consistent calculations) for $w = 20$ and 70 nm as insets; $\tilde{w}$ is defined as the standard deviation of the charge distribution from its center. The black symbol is $^{1/3}\Delta$ by Suen *et al.* [39] for a 2DES with similar density to ours and $w = 77$ nm. For $w = 80$ nm, we find an insulating phase instead of a FQHE and represent it with an open circle. The data show a clear decrease of $^{1/3}\Delta$ with increasing layer thickness (the dashed line drawn for $20 \leq w \leq 70$ is a least-squares fit through the data points).

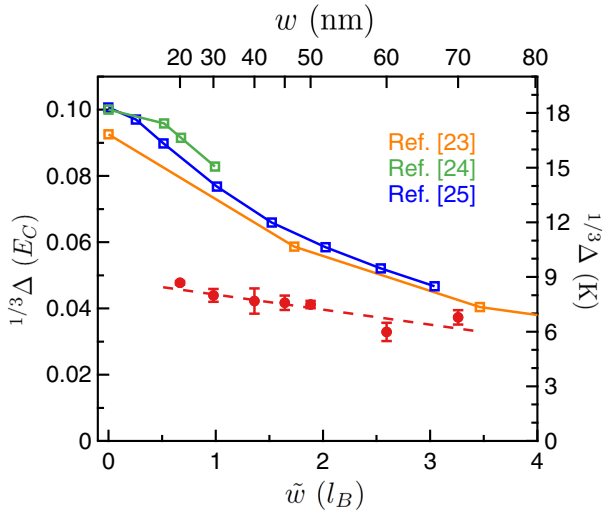

FIG. 3. $^{1/3}\Delta$ versus $\tilde{w}$. The open symbols are from theoretical calculations that include the role of finite layer thickness [24,25], and Landau level mixing and finite layer thickness [23].

2DESs [22–25,30–32]. We emphasize that our result is the first report of $^{1/3}\Delta$ versus $\tilde{w}$ that keeps LLM and l_B fixed so as to elucidate the quantitative role of layer thickness. Note, however, that another parameter that affects $^{1/3}\Delta$, namely disorder, could vary between our different samples; we will return to this later in the Letter.

When $w > 70$ nm, the $\nu = 1/3$ FQHE becomes very weak quickly and $^{1/3}\Delta$ eventually vanishes. In Fig. 2 we have included a data point at $w = 77$ nm from Suen *et al.* [39]. For larger w, in sample S_{80}, we observe an insulating phase instead of a $\nu = 1/3$ FQHE. Such an insulating phase appears when the charge distribution in wide QWs becomes predominantly bilayerlike [39–41]. As detailed elsewhere, the insulating phase signals a correlated, *bilayer* Wigner crystal state [40–43]. In Fig. 2, we represent this vanishing of the FQHE in sample S_{80} by an open circle for $w = 80$ nm ($\tilde{w} \simeq 4.0$). We report the energy gaps as a function of $\tilde{w}$ for FQHE at $\nu = 2/3$, $2/5$, and $3/5$ in the SM [37].

For a quantitative comparison with the results of calculations, in Fig. 3 we plot the measured $^{1/3}\Delta$ versus $\tilde{w}$ and, using open squares, we also present the energy gaps calculated in three different studies, all of which assume zero disorder. The green and blue symbols represent calculations that include only the role of layer thickness [24,25], while the orange symbols include both layer thickness and LLM [23]. In Fig. 3 we present Ref. [23] results for LLM parameter $\kappa \simeq 0.68$, which is equal to κ in our samples; also note that this value of κ reduces the calculated $^{1/3}\Delta$ from $\simeq 0.10 E_C$ to $\simeq 0.09 E_C$ at $\tilde{w} = 0$, as seen in Fig. 3. References [24,25] computed the Coulomb potential in a local-density approximation for 2DESs confined to QWs, while in Ref. [23] the Zhang–Das Sarma potential [22] for 2DESs confined to heterojunctions was used. There is an overall, qualitative agreement in Fig. 3 between the experimental and theoretical results in that both exhibit a decrease with increasing $\tilde{w}$. However, the experimental data uniformly fall below calculations, with the difference being largest at the smallest $\tilde{w}$.

Since one possible source for the discrepancy is the presence of disorder, we attempt to extract an experimental estimate for the role of disorder in lowering $^{1/3}\Delta$ in our samples. We do this by considering the energy gaps $^{\nu}\Delta$ for higher-order FQHE states at other ν near $\nu = 1/2$. For an ideal 2DES, these gaps are expected to scale as $^{\nu}\Delta = (C/|2p+1|)E_C$ [3,44], where $C \simeq 0.3$ and $\nu = p/(2p+1)$. Figure 4 displays $^{\nu}\Delta$ versus $(e^2/4\pi\epsilon_0\epsilon l_B)/(2p+1)$ (red symbols) for sample S_{70} for ν up to $8/17$ and $8/15$. In Fig. 4, we also show red lines representing fits to the measured gaps. The magnitude of the negative intercepts of these lines with the y axis is generally believed to provide an estimate of the disorder energy, Γ, based on the assumption that disorder reduces the gaps for different FQHE states by a fixed amount equal to Γ [20,21,45]. For the data of Fig. 4, we find $\Gamma = (1.2 \pm 0.2)$ K; this is approximately half the previous values in 2DESs [20,21] and 2D hole systems [45], and is about an order of magnitude smaller than in graphene [46], attesting to the extremely high quality of our 2DESs.

In Fig. 4, the data plotted by red symbols and the fitted lines are not symmetric with respect to the y axis while

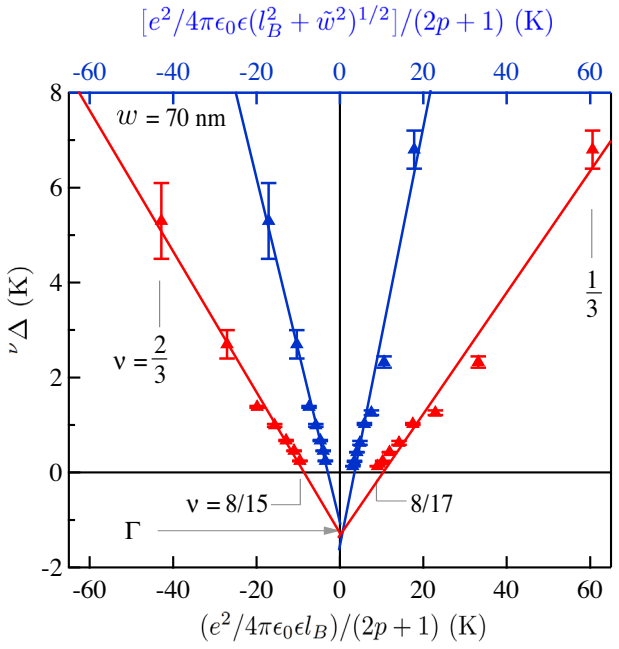

FIG. 4. Red symbols are $^{\nu}\Delta$ versus $(e^2/4\pi\epsilon_0\epsilon l_B)/(2p+1)$, for a 2DES with $w = 70$ nm. The ν range is from 1/3 to 8/17, and 2/3 to 8/15. The red lines are linear fits to the data. The blue symbols are $^{\nu}\Delta$ versus the Zhang–Das Sarma energy $[e^2/4\pi\epsilon_0\epsilon(l_B^2+\tilde{w}^2)^{1/2}]/(2p+1)$. The blue lines are linear fits to the blue data points. The red and blue lines have negative intercept values with the y axis that we identify as the phenomenological disorder parameter (Γ).

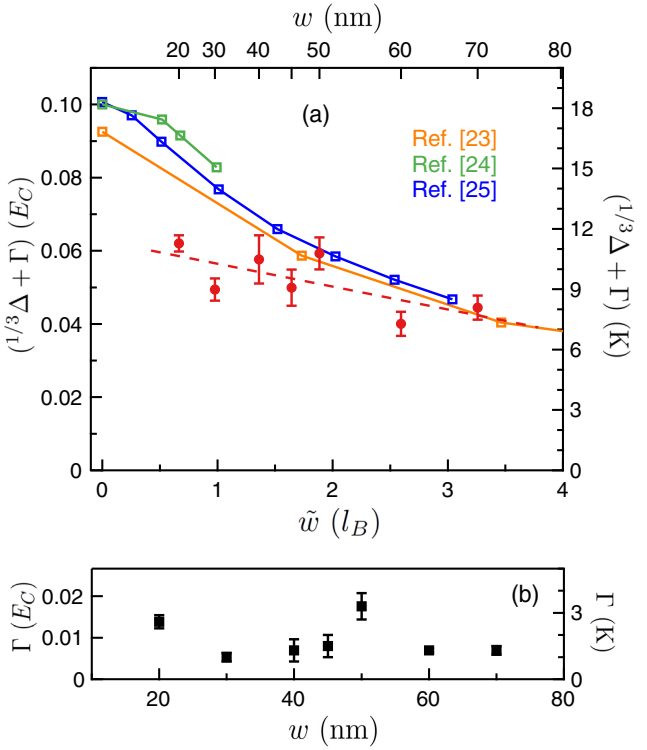

FIG. 5. (a) Closed red symbols are the measured $^{1/3}\Delta$ with the added corresponding Γ parameter to account for disorder. (b) The parameter Γ versus w. The adjusted measured gaps in (a) are overall in better agreement with the calculations, but have larger uncertainties and scatter (compared to Fig. 3) because of the scatter and uncertainties in values of Γ.

theoretically, for an ideal 2DES, they should be symmetric. The asymmetry can be readily attributed to the finite layer thickness of the 2DES: since l_B changes with B, so does $\tilde{w}$, implying that the 2DES is effectively wider at higher B, or equivalently at smaller ν. To account for the changes in $\tilde{w}$ as a function ν, we plot our measured gaps versus the Zhang–Das Sarma energy $[e^2/4\pi\epsilon_0\epsilon(l_B^2+\tilde{w}^2)^{1/2}]/(2p+1)$ [22] (top axis and blue symbols in Fig. 4). Because of the reduced Coulomb interaction, the blue symbols cover a smaller range in the x axis compared to the red symbols. The data are now much more symmetric with respect to the y axis, as also clearly seen from the blue lines that are fits through the data points. The average of the intercepts of these lines with the y axis yields $\Gamma = (1.3 \pm 0.2)$ K, slightly larger than Γ deduced from the red lines. Plots similar to Fig. 4 are reported in the SM [37] for the other samples in our study.

In Fig. 5(b) we summarize the measured Γ versus $\tilde{w}$, deduced from analyses similar to the one shown in Fig. 4, for all the samples in our study [37]. For Γ we use the average of values deduced from the intercepts of the blue lines with the y axis in Fig. 4. Note that the measured Γ are typically a very small fraction ($\simeq$1%) of the Coulomb energy, attesting to the very low disorder in our samples. On the other hand, Γ values are not negligible compared to $^{1/3}\Delta$. Moreover, there is significant experimental uncertainty and scatter in values of Γ. More importantly, the measured Γ do not correlate with the amount of disorder expected from the sample mobilities [Fig. 1(a)]. For example, the sample with a 50-nm-wide well width has the highest mobility among all the samples [Fig. 1(a)], but it exhibits the largest Γ in Fig. 5(b), implying the highest disorder. This lack of a clear correlation between the experimentally observed strengths of FQHE states and the transport mobilities, which are measured at zero magnetic field, was first noted in Ref. [47], and remains to be explained rigorously.

With the above caveats regarding the values of Γ in mind, it is nevertheless instructive to add the deduced Γ to the measured $^{1/3}\Delta$ to assess the role of disorder in affecting the energy gaps in an approximate manner. The data are shown in Fig. 5(a). With the added Γ, the adjusted energy gaps exhibit more scatter compared to the experimental gaps shown in Figs. 2 and 3; this can be attributed mostly to the scatter of Γ, as seen in Fig. 5(b). Despite the extra scatter, it is clear that the energy gaps decrease with increasing layer thickness. The dashed line (a least-squares fit to the data) has a negative slope supporting this statement; the magnitude of the slope is even larger than in Figs. 2 and 3 fittings. Also, the adjusted gaps are overall closer to the theoretical

calculations, although they still fall below the calculated values at small layer thicknesses.

To summarize, we present the first systematic experimental study of the dependence of the $\nu = 1/3$ FQHE energy gap on the electron layer thicknesses in very high-quality 2DESs confined to GaAs QWs. There is a clear decrease of the gap with increasing layer thickness (Fig. 2), qualitatively consistent with the results of available calculations. However, the experimental gaps are noticeably smaller than the calculated values, particularly for smaller electron layer thicknesses (Fig. 3). Accounting for the role of disorder in a phenomenological fashion, the adjusted gaps are in better overall agreement with the calculations (Fig. 5), although they exhibit additional scatter stemming from the uncertainty in how the disorder is evaluated. For a closer, more quantitative comparison of the experimental and theoretical results, a more rigorous method for incorporating the role of disorder, both experimentally and theoretically, is necessary. Also, future calculations based on parameters that better match those of our samples would be welcome. For example, calculations in Ref. [23], which do take LLM into account, use a charge distribution which is appropriate for a triangular confinement (GaAs/AlGaAs heterojunction) but not for a QW with a square potential. We hope that our systematic experimental data, taken in extremely high-quality 2DESs, would stimulate future theoretical calculations relevant to the parameters of our samples.

We acknowledge support by the National Science Foundation (NSF) Grants No. DMR 1709076 and No. DMR 2104771 for measurements. For sample synthesis and characterization, we acknowledge support by NSF Grants No. ECCS 1906253 and No. MRSEC DMR 1420541, and the Gordon and Betty Moore Foundation's EPiQS Initiative (Grant No. GBMF9615 to L. N. P.). This research is funded in part by QuantEmX Travel Grants from the Institute for Complex Adaptive Matter. A portion of this work was performed at the National High Magnetic Field Laboratory (NHMFL), which is supported by National Science Foundation Cooperative Agreement No. DMR-1644779 and the state of Florida. We thank S. Hannahs, T. Murphy, A. Bangura, G. Jones, and E. Green at NHMFL for technical support. We also thank J. K. Jain for illuminating discussions.

[1] D. C. Tsui, H. L. Stormer, and A. C. Gossard, Two-Dimensional Magnetotransport in the Extreme Quantum Limit, Phys. Rev. Lett. **48**, 1559 (1982).

[2] *Perspective in Quantum Hall Effects: Novel Quantum Liquids in Low-Dimensional Semiconductor Structures*, edited by S. Das Sarma and A. Pinczuk (Wiley, New York, 1997).

[3] J. K. Jain, *Composite Fermions* (Cambridge University Press, Cambridge, England, 2007).

[4] *Fractional Quantum Hall Effects: New Developments*, edited by B. I. Halperin and J. K. Jain (World Scientific, Singapore, 2020).

[5] K. von Klitzing, T. Chackraborty, P. Kim, V. Madhavan, X. Dai, J. Mclver, Y. Tokura, L. Savary, D. Smirnova, A. Maria Rey, C. Felser, J. Gooth, and X. Qi, 40 years of the quantum Hall effect, Nat. Rev. Phys. **2**, 397 (2020).

[6] F. D. M. Haldane, Nobel lecture: Topological quantum matter, Rev. Mod. Phys. **89**, 040502 (2017).

[7] C. Nayak, S. H. Simon, A. Stern, M. Freedman, and S. Das Sarma, Non-Abelian anyons and topological quantum computation, Rev. Mod. Phys. **80**, 1083 (2008).

[8] R. S. Mong, D. J. Clarke, J. Alicea, N. H. Lindner, P. Fendley, C. Nayak, Y. Oreg, A. Stern, E. Berg, K. Shtengel, and M. P. Fisher, Universal Topological Quantum Computation from a Supercondcutor-Abelian Quantum Hall Heterostructure, Phys. Rev. X **4**, 011036 (2014).

[9] Ö. Gül, Y. Ronen, S. Y. Lee, H. Shapourian, J. Zauberman, Y. H. Lee, K. Watanabe, T. Taniguchi, A. Vishwanath, A. Yacoby, and P. Kim, Induced superconductivity in the fractional quantum Hall edge, arXiv:2009.07836.

[10] R. de Picciotto, M. Reznikov, M. Heiblum, V. Umansky, G. Bunin, and D. Mahalu, Direct observation of a fractional charge, Nature (London) **389**, 162 (1997).

[11] L. Saminadayar, D. C. Glattli, Y. Jin, and B. Etienne, Observation of the $e/3$ Fractionally Charged Laughlin Quasiparticle, Phys. Rev. Lett. **79**, 2526 (1997).

[12] J. Nakamura, S. Fallahi, H. Sahasrabudhe, R. Rahman, S. Lian, G. C. Gardner, and M. J. Manfra, Aharonov Bohm interference of fractional quantum Halll edge modes, Nat. Phys. **15**, 563 (2019).

[13] J. Nakamura, S. Liang, G. C. Gardner, and M. J. Manfra, Direct observation of anyonic braiding statistics, Nat. Phys. **16**, 931 (2020).

[14] H. Bartolomei, M. Kumar, R. Bisognin, A. Marguerite, J. M. Berroir, E. Bocquillon, B. Placais, A. Cavanna, Q. Dong, U. Gennser, Y. Jin, and G. Feve, Fractional statistics in anyon collisions, Science **368**, 173 (2020).

[15] R. Morf and B. I. Halperin, Monte Carlo evaluation of trial wave functions for the fractional quantized Hall effect: Disk geometry, Phys. Rev. B **33**, 2221 (1986).

[16] F. D. M. Haldane and E. H. Rezayi, Finite-Size Studies of the Incompressible State of the Fractionally Quantized Hall Effect and Its Excitations, Phys. Rev. Lett. **54**, 237 (1985).

[17] S. M. Girvin, A. H. MacDonald, and P. M. Platzman, Collective-Excitation Gap in the Fractional Quantum Hall Effect, Phys. Rev. Lett. **54**, 581 (1985).

[18] G. S. Boebinger, A. M. Chang, H. L. Stormer, and D. C. Tsui, Magnetic Field Dependence of Activation Energies in the Fractional Quantum Hall Effect, Phys. Rev. Lett. **55**, 1606 (1985).

[19] R. L. Willett, H. L. Stormer, D. C. Tsui, A. C. Gossard, and J. H. English, Quantitative experimental test for the theoretical gap energies in the fractional quantum Hall effect, Phys. Rev. B **37**, 8476 (1988).

[20] R. R. Du, H. L. Stormer, D. C. Tsui, L. N. Pfeiffer, and K. W. West, Experimental Evidence for New Particles in the Fractional Quantum Hall Effect, Phys. Rev. Lett. **70**, 2944 (1993).

[21] W. Pan, W. Kang, M. Lilly, J. Reno, K. Baldwin, K. West, L. Pfeiffer, and D. Tsui, Particle-Hole Symmetry and the Fractional Quantum Hall Effect in the Lowest Landau Level, Phys. Rev. Lett. **124**, 156801 (2020).
[22] F. C. Zhang and S. Das Sarma, Excitation gap in the fractional quantum Hall effect: Finite layer thickness corrections, Phys. Rev. B **33**, 2903 (1986).
[23] V. Melik-Alaverdian and N. E. Bonesteel, Composite fermions and Landau-level mixing in the fractional quantum Hall effect, Phys. Rev. B **52**, R17032 (1995).
[24] K. Park, N. Meskini, and J. K. Jain, Activation gaps for the fractional quantum Hall effect: Realistic treatment of transverse thickness, J. Phys. Condens. Matter **11**, 7283 (1999).
[25] R. H. Morf, N. d'Ambrumenil, and S. Das Sarma, Excitation gaps in fractional quantum Hall states: An exact diagonalization study, Phys. Rev. B **66**, 075408 (2002).
[26] D. Yoshioka, Effect of the Landau level mixing on the ground state of two-dimensional electrons, J. Phys. Soc. Jpn. **53**, 3740 (1984).
[27] D. Yoshioka, Effect of higher Landau levels on the excitation spectrum of the ground state of 2D electrons, Surface Sci. **170**, 125 (1986).
[28] A. Gold, Excitation gap in the fractionally quantized Hall effect, Phys. Rev. B **36**, 3268 (1987).
[29] P. M. Platzman, dc conductivity and gap energies in the fractional quantum Hall effect, Phys. Rev. B **39**, 7985 (1989).
[30] M. Shayegan, J. Jo, Y. W. Suen, M. Santos, and V. J. Goldman, Collapse of the Fractional Quantum Hall Effect in an Electron System with Large Layer Thickness, Phys. Rev. Lett. **65**, 2916 (1990).
[31] S. He, F. C. Zhang, X. C. Xie, and S. Das Sarma, Destruction of fractional quantum Hall effect in thick systems, Phys. Rev. B **42**, 11376 (1990).
[32] V. Halonen, Collapse of the fractional quantum Hall effect in a parabolic quantum well, Phys. Rev. B **47**, 10001 (1993).
[33] Y. J. Chung, K. A. Villegas Rosales, K. W. Baldwin, K. W. West, M. Shayegan, and L. N. Pfeiffer, Working principles of doping-well structures for high-mobility two-dimensional electron systems, Phys. Rev. Mater. **4**, 044003 (2020).
[34] J. M. Li, J. J. Wu, X. X. Han, Y. W. Lu, X. L. Liu, Q. S. Zhu, and Z. G. Wang, A model for scattering due to interface roughness in finite quantum wells, Semicond. Sci. Technol. **20**, 1207 (2005).
[35] D. Kamburov, K. W. Baldwin, K. W. West, M. Shayegan, and L. N. Pfeiffer, Interplay between quantum well width and interface roughness for electron transport mobility in GaAs quantum wells, Appl. Phys. Lett. **109**, 232105 (2016).
[36] H. Stormer, A. C. Gossard, and W. Wiegmann, Observation of intersubband scattering in a two-dimensional electron system, Solid State Commun. **41**, 707 (1982).
[37] See Supplemental Material at http://link.aps.org/supplemental/10.1103/PhysRevLett.127.056801 for other samples and other FQHE states (at $\nu = 2/3$, $2/5$, and $3/5$).
[38] R. Martin, 2D Schroedinger-Poisson solver AQUILA, Library Catalog, www.mathworks.com.
[39] Y. W. Suen, H. C. Manoharan, X. Ying, M. B. Santos, and M. Shayegan, Origin of the $\nu = 1/2$ Fractional Quantum Hall State in Wide Single Quantum Wells, Phys. Rev. Lett. **72**, 3405 (1994).
[40] Y. W. Suen, L. W. Engel, M. B. Santos, M. Shayegan, and D. C. Tsui, Observation of a $\nu = 1/2$ Fractional Quantum Hall State in a Double-Layer Electron System, Phys. Rev. Lett. **68**, 1379 (1992).
[41] H. C. Manoharan, Y. W. Suen, M. B. Santos, and M. Shayegan, Evidence for a Bilayer Quantum Wigner Solid, Phys. Rev. Lett. **77**, 1813 (1996).
[42] A. T. Hatke, Y. Liu, L. W. Engel, M. Shayegan, L. N. Pfeiffer, K. W. West, and K. W. Baldwin, Microwave spectroscopy of the low-filling-factor bilayer electron solid in a wide quantum well, Nat. Commun. **6**, 7071 (2015).
[43] A. T. Hatke, Y. Liu, L. W. Engel, L. N. Pfeiffer, K. W. West, K. W. Baldwin, and M. Shayegan, Microwave spectroscopic observation of a Wigner solid within the $\nu = 1/2$ fractional quantum Hall effect, Phys. Rev. B **95**, 045417 (2017).
[44] B. I. Halperin, P. A. Lee, and N. Read, Theory of the half-filled Landau level, Phys. Rev. B **47**, 7312 (1993),
[45] H. C. Manoharan, M. Shayegan, and S. J. Klepper, Signatures of a Novel Fermi Liquid in a Two-Dimensional Composite Particle Metal, Phys. Rev. Lett. **73**, 3270 (1994).
[46] H. Polshyn, H. Zhou, E. Spanton, T. Taniguchi, K. Watanabe, and A. Young, Quantitative Transport Measurements of Fractional Quantum Hall Energy Gaps in Edgeless Graphene Devices, Phys. Rev. Lett. **121**, 226801 (2018).
[47] T. Sajoto, Y. W. Suen, L. W. Engel, M. B. Santos, and M. Shayegan, Fractional quantum Hall effect in very-low-density $GaAs/Al_xGa_{1-x}As$ heterostructures, Phys. Rev. B **41**, 8449 (1990).